Investigational Studies on a Hit Compound Cyclopropane-Carboxylic Acid Derivative Targeting O-Acetylserine Sulfhydrylase as a Colistin Adjuvant

Investigational studies on a hit compound cyclopropane-carboxylic acid derivative targeting *O*-acetylserine sulfhydrylase as colistin adjuvant

Giannamaria Annunziato[a,°,], Costanza Spadini[b,°], Nina Franko[c], Paola Storici[d], Nicola Demitri[d], Marco Pieroni[a], Sara Flisi[b], Lucrezia Rosati[b], Mattia Iannarelli[b], Marialaura Marchetti[f], Joana Magalãesh[a], Stefano Bettati[e,f,g], Andrea Mozzarelli[c,f,g], Clotilde Silvia Cabassi[b], Barbara Campanini[c,f], Gabriele Costantino[a].*

[a] *P4T group, Department of Food and Drugs, University of Parma, Parco Area delle Scienze 27/A, 43124 Parma, Italy.*

[b] *Operative Unit of Animals Infectious Diseases, Department of Veterinary Science, University of Parma, via del Taglio, 8, 43126 Parma, Italy.*

[c] *Laboratory of Biochemistry and Molecular Biology, Department of Food and Drugs, University of Parma, via Parco Area delle Scienze 23/A, 43124 Parma, Italy.*

[d] *Elettra - Sincrotrone Trieste S.C.p.A., SS 14 - km 163,5 in AREA Science Park 34149 Trieste, Italy.*

[e] *Department of Medicine and Surgery, University of Parma, via Volturno, 39, 43125 Parma, Italy.*

[f] *Biopharmanet-TEC Interdepartmental Center, University of Parma, 43124 Parma, Italy.*

[g] *Institute of Biophysics, CNR, 56124 Pisa, Italy.*

° equally contributed

* corresponding author: giannamaria.annunziato@unipr.it

Abstract

Antibacterial adjuvants are of great significance since they allow to lowering the therapeutic dose of conventional antibiotics and to reduce the impact of antibiotic resistance. Herein we report that *O*-acetylserine sulfhydrylase (OASS) inhibitors can be used as colistin adjuvants to treat infections caused by Gram-positive and Gram-negative pathogens. A compound that binds OASS with nM

dissociation constant was tested as adjuvant of colistin against six critical pathogens responsible for infections spreading worldwide, *Escherichia coli*, *Salmonella enterica* serovar Typhimurium, *Klebisiella pneumoniae*, *Staphylococcus aureus*, *methicillin resistant Staphylococcus aureus* and *Staphylococcus pseudintermedius*. The compound showed promising synergistic and additive activities against all of them. Knock-out experiments confirmed the intracellular target engagement supporting the proposed mechanism of action. Moreover, compound toxicity was evaluated by means of its haemolytic activity against sheep defibrinated blood cells, showing a good safety profile. The 3D structure of the compound in complex with OASS was determined at 1.2 Å resolution by macromolecular crystallography providing for the first time structural insights about the nature of the interaction between the enzyme and this class of competitive inhibitors. Our results provide a robust proof of principle supporting OASS as a potential non-essential antibacterial target to develop a new class of adjuvants and the structural basis for further structure-activity relationship studies.

KEYWORDS

Antibiotic adjuvants, colistin adjuvants, bacterial non-essential pathways, sulfur assimilation pathway, *O*-acetylserine sulfhydrylase inhibitors.

INTRODUCTION

The discovery of antimicrobial drugs made possible significant scientific progresses in medicine and agricultural fields in the past century.[1] Unfortunately, the misuse and overuse of antibiotics have led to the emergence of multidrug resistant (MDR) and extensively drug resistant (XDR) bacteria.[2] Infections caused by resistant pathogens are difficult to treat and often require more costly and toxic alternatives to drugs commonly used in therapy.[3] The expectations for the future are not

encouraging and issues related to antimicrobial resistance (AMR) are expected to increase if greater efforts will not be made to preserve currently available drugs and to intensify the search for new antimicrobial agents.[2] In this regard, a promising strategy is the use of combination therapies aimed at lowering the required antibiotic dosage, and, in turn, leading to the reduction of the occurrence of adverse events and of the development of resistance. It has already been proven that the use of antibiotic adjuvants is a winning strategy in (*i*) fighting MDR and XDR bacteria and (*ii*) improving the safety profile of antibiotics endowed with narrow therapeutic window, allowing for the preservation of the already existing antibacterial drug arsenal.[4] Adjuvants are molecules with weak or absent antimicrobial activity that, when used in association with antibiotics, can lead to an enhancement of the antibiotic activity by minimizing or blocking resistance and/or by reducing the clinical dosage at which the therapeutic effects is obtained.[5] Among others, one of the most successful examples is the combination of amoxicillin and clavulanic acid, which led to the commercialization of co-amoxiclav.[6] Another relevant example is the association of sulfamethoxazole and trimethoprim which are both antimetabolites and exert their action by decreasing the synthesis of the essential metabolite folic acid.[7] Bacterial metabolic pathways represent a still underexploited reservoir of potential targets for enhancers of antimicrobial therapy. The non-essentiality of such targets for microbial survival outside the infection setting [8,9] would in principle reduce the risk of the emergence of resistance. In this context, among new possible pathways endowed with non-essential targets described in literature,[10] the cysteine biosynthesis pathway, also known as sulfur assimilation pathway, turned out to be of great interest.[11] In the past 10 years our group [12–19] and others [20,21] have developed inhibitors of the biosynthesis of cysteine in bacteria and mycobacteria for application as antibiotics/enhancers of antibiotic therapy. Cysteine is a building block for all sulfur-containing biomacromolecules that are crucial for living organisms and is produced by bacteria and plants through the reductive sulfate assimilation pathway using inorganic sulfur

(mainly sulfate and thiosulfate).[22] Mammals produce cysteine from the essential amino acid methionine and lack all the enzymes of the sulfur assimilation pathway.[23] The last two steps of cysteine biosynthesis in bacteria are catalyzed by the enzymes serine acetyltransferase (SAT) and *O*-acetylserine sulfhydrylase (OASS), respectively. The first enzyme catalyzes the activation of serine to *O*-acetylserine (OAS), which is then converted to cysteine by the enzymatic activity of OASS. These two enzymes can assemble in the so-called "cysteine synthase complex" (CSC) that is stabilized through the interaction between the C-terminal sequence of SAT and the active site of OASS.[24–26]

In most bacteria, at least two OASS isoforms exist, showing a high level of homology and peculiar functional and structural properties: OASS-A, encoded by *cysK*, and OASS-B, encoded by *cysM*. In bacteria, both isozymes use OAS as the first substrate and bisulfide as a sulfur source. In addition to bisulfide, OASS-B can also use thiosulfate. OASS-A and OASS-B are differently expressed under aerobic/anaerobic conditions; however, little is known about their respective roles under infection conditions. For this reason, the identification of small-molecules able to inhibit the activity of both OASS isoforms is of great interest.[27]

In our previous works we have initiated a program directed to the design and synthesis of novel substituted cyclopropane-carboxylic acids, aimed at improving their activity toward both OASS-A and OASS-B isoforms. In particular, we were pleased to notice that, to the best of our knowledge, **UPAR415** (**Figure 1**)[15] has been found as the most potent inhibitor towards both isoforms with a K_D in the low nanomolar range.[12–15,18,28]

One of the most interesting results reported in literature about the phenotypic effects of the inhibition of bacterial biosynthesis of cysteine is the effect on antibiotic resistance. Investigations on deletion mutants of this pathway in *Salmonella enterica* serovar Typhimurium led to the conclusion that unpaired oxidative stress response, due to inactivation of cysteine biosynthesis,

causes a decrease in antibiotic resistance in both vegetative and swarm cell populations, and, most interestingly, conventional antibiotics are effective at lower doses.[29] These findings suggest that inhibitors of cysteine biosynthesis could enhance the efficacy of antibiotic treatment, decreasing the spreading of resistance and allowing the use of antibiotics at a lower dosage. Based on such observation, it is plausible that chemical inhibition of OASS isoforms represents a good approach for the development of enhancers of antibiotic therapy.

Among the antibiotics belonging to the drug arsenal used to treat resistant bacterial infections, colistin is considered a last-resort molecule, used to treat severe infections caused by MDR and XDR bacteria.[30] In this frame, colistin is viewed by the World Health Organization (WHO) as the last-resort treatment to deal with serious antimicrobial resistant infections in patients in critical conditions.

Colistin, together with polymyxins, belongs to the class of glycopeptide antibiotics that is produced by *Bacillus* polymixa var. *colistinus.*[31] The colistin bactericidal effect is reached through the interaction with components of the outer membrane of Gram-negative bacteria.[32] Indeed, by binding to lipopolysaccharides (LPSs) and phospholipids of the outer cell membrane it competitively displaces divalent cations (Ca^{2+} and Mg^{2+}) from the phosphate groups of membrane lipids. This leads to disruption of the outer cell membrane, leakage of intracellular contents and bacterial death.[33]

Due to its mechanism of action, colistin is not devoided of severe adverse effects, including nephrotoxicity and neurotoxicity, which hampered its clinical use.[34] Indeed, after almost a decade since its discovery, colistin was replaced by other antibiotics. Nevertheless, the spreading of MDR and XDR bacteria, especially those belonging to the ESKAPE group, has led to the renaissance of the worldwide colistin clinical use.[2]

We thus decided (*i*) to challenge **UPAR415** as potential colistin adjuvant against different pathogenic bacteria *in vitro*, (*ii*) to provide, by using *cysK* and *cysM* knock-out *S.* Typhimurium strains, a proof

of principle that **UPAR415** exerts its in-vitro activity through the inhibition of both OASS isoforms, and (*iii*) to disclose the structural details underlying OASS inhibition by X-ray crystallography.

RESULTS AND DISCUSSION

The bacteria chosen for testing the potential application of **UPAR415 (Figure 1)** as a colistin adjuvant were: *E. coli*, *S.* Typhimurium, *K. pneumoniae*, *S. aureus*, methicillin resistant *S. aureus* (MRSA) and *S. pseudintermedius*.

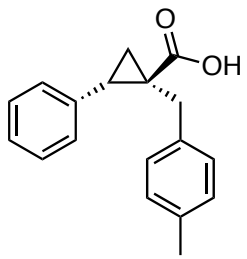

(1*S*,2*S*)-1-(4-methylbenzyl)-2-phenylcyclopropanecarboxylic acid

UPAR415

Figure 1. Chemical structure of **UPAR415**.

This choice was dictated by the following reasons: (i) they are important, worldwide distributed, human opportunistic pathogens which often cause resistant infections; (ii) some of them are part of the ESKAPE group and the antibiotic treatments for these infections are usually aggressive, toxic, and largely inefficient; (iii) according to the literature and to our previous works in this field, there is evidence that the enzymes of the sulfur assimilation pathway, and in particular OASS, are expressed in the aforementioned pathogens and might be involved in the mechanisms of antibiotic resistance. The existence of the genes coding for the enzymes involved in sulfur assimilation has been confirmed for all the six pathogens either by published studies[35,36] or by homology in UniProtKB and Kegg Pathways databases.[37] However, whereas in Gram-negative bacteria the two OASS-A and OASS-B isozymes are present, in Gram-positive the existence of isozymes with distinct

substrate preferences or expression patterns has never been thouroughly investigated. In *S. aureus* an *O*-acetylserine sulfhydrylase with higher sequence identity to CysK but able to use thiosulfate as substrate has been described. [38] In **Figure 2** the sequence alignment of *Salmonella* CysK with homologs from Gram-positive and Gram-negative bacteria is shown. The active site residues are strictly conserved, except for Ile230 that, however, underwent a conservative substitution to leucine in *Staphylococcus spp*. This indicates that molecules developed against *Salmonella* CysK should in principle bind with comparable affinity to the orthologs from different species.

Indeed, while *S.* Typhimurium was considered as a model for computational studies, target engagement validation and crystallographic investigations, in most cases the results obtained could be expanded to other pathogens of great clinical interest.

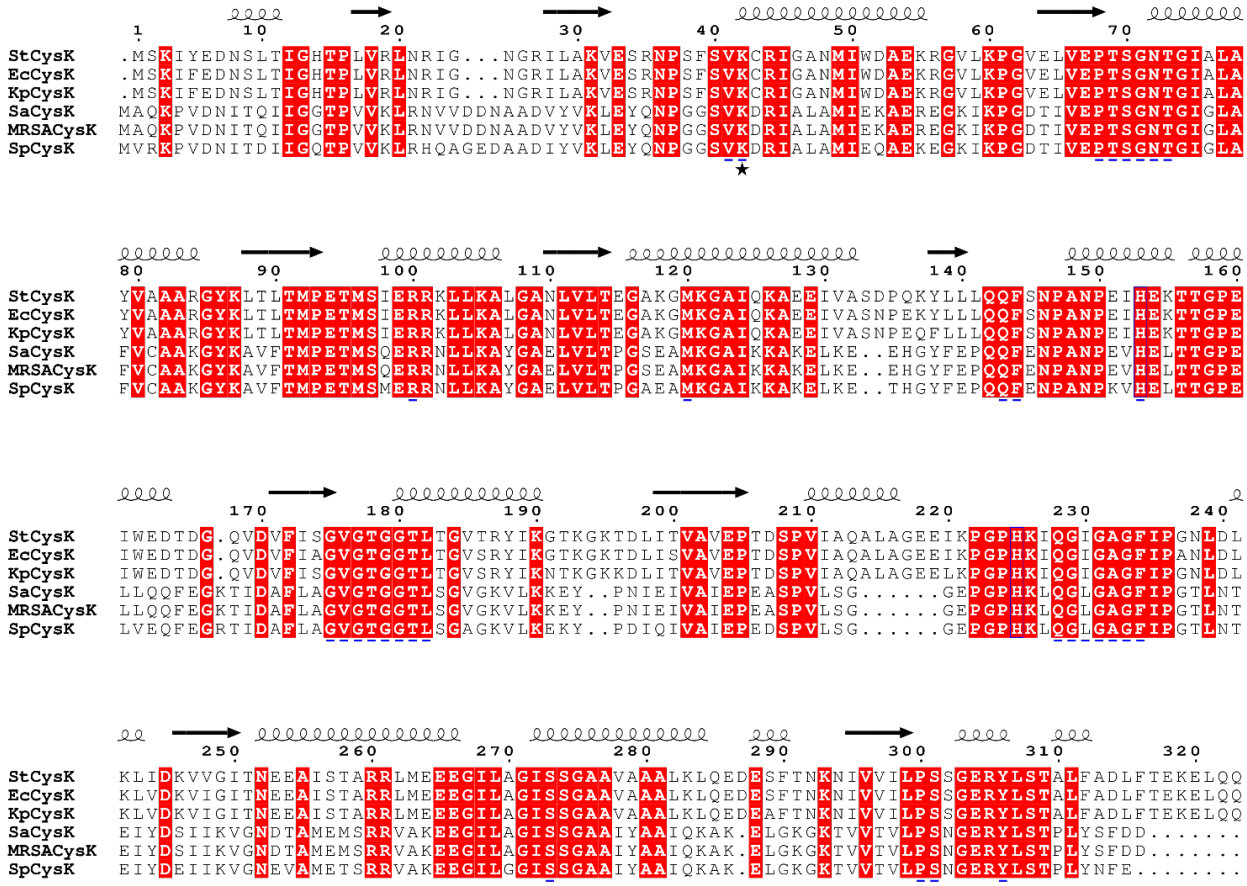

Figure 2. The alignment of the amino acid sequences of CysK from Gram-negative (*Salmonella*, StCysK; *E. coli*, EcCysK*; K. pneumoniae*, KpCysK) and Gram-positive (*S. aureus*, SaCysK; MRSA, MRSACysK; *S. pseudintermedius*, SpCysK) bacteria.

Alignment was performed using the Clustal Omega program[39] (running on UniProtKB). Similarity scores were calculated by the ESPript program[40] using the Blosum62 matrix set at default global score. Residues of the active site are marked with a blue dash below the alignment. The active site lysine is marked with a star. The secondary structure elements depicted on the top of the alignment are taken from PDB entry 1OAS.

Inhibition activity profiling on pathogen cells growth *in-vitro*

We decided to test **UPAR415** into a multi-step pipeline. We firstly evaluated the activity of **UPAR415** alone against six representative pathogens (**Table 1**). In a rich medium, where cysteine is largely available and its biosynthesis is thus inhibited, OASS is a dispensable enzyme and its chemical inhibition should not affect bacterial cell growth and survival. On the other hand, testing OASS inhibitors in a rich medium would be of poor significance for the purpose of this study. In fact, the cysteine present in the growth medium would be transported inside the cells, thus reversing the inhibition of its biosynthesis. Therefore, minimal inhibitory concentrations (MICs) were evaluated both in conventional Müller-Hinton broth (MHB) and in minimal media (20% LB) with a limited amount of nutrients, where cysteine is present at a lower concentration, and thus the effect of inhibiting its biosynthesis would lead to growth-inhibiting effects. In line with this reasoning, the data reported in **Table 1** show that **UPAR415**, used alone, does not possess bactericidal or bacteriostatic effects on most of the tested strains and only negligible effects on *S*. *aureus* and *S. pseudintermedius* in both media.

Bacterial strains	**MIC (µg/ml)**	
	MHB	**20% LB**
***E. coli* ATCC25922**	>256	>256
S. T*yphimurium* ATCC14028	>256	>256
***K. pneumoniae* ATCC13883**	>256	>256

S. aureus	128	107
MRSA	>256	>256
S. pseudintermedius	111	136

Table 1. MIC of **UPAR415** tested alone against six different pathogens. *MIC was measured on MHB broth or 20% LB.*

In order to rule out the possibility that these data are due to a likely possibility that **UPAR415** does not pentretate into Gram-negative cells, we used PMBN as a non-antibiotic membrane permeabilzer. To this purpose, UPAR415 was used in combination with Polimixin B nonapeptide (PMBN),[41] a membrane destabilizer, lacking of antibacterial activity. Even in this case, no appreciable MIC is observed (See Supplementary Table S1), supporting the notion that (*i*) **UPAR415** has no antibactierial activity *per se*, and (*ii*) the lack of activity of **UPAR415** in cells growing *in vitro* is not linked to penetration/accumultion issues but rather to the fact that the compound exerts its activity only as colistin adjuvant. Instead, when administered as colistin adjuvant, **UPAR415** reduces the level of cell growth, in some cases even at the lower concentrations tested.

Having thus excluded that **UPAR415** behaves as an antibacterial agent in its own, we decided to further evaluate it as an adjuvant in combination with colistin, to get clues about their potential synergistic, additive, or antagonistic interactions.

Combination with Colistin

UPAR415 was tested in combination with colistin at different concentrations on both MHB and 20% LB, to assess any effect of cysteine availability.

A strong effect can be observed when **UPAR415** is used at 32 μg/ml and 64 μg/ml in association with colistin on *K. pneumoniae* cells growing *in vitro*. In this condition the MIC of colistin becomes seven times lower with respect to when administered alone. It is possible to see the same trend

with the other Gram-negative bacteria tested, indeed a 2.5-fold decrease in MIC is observed in *E. coli* when colistin is tested in the presence of **UPAR415** at 64 µg/ml. In the case of *Salmonella* the MIC in the presence of 32 µg/ml **UPAR415** decreases more than 4-fold.

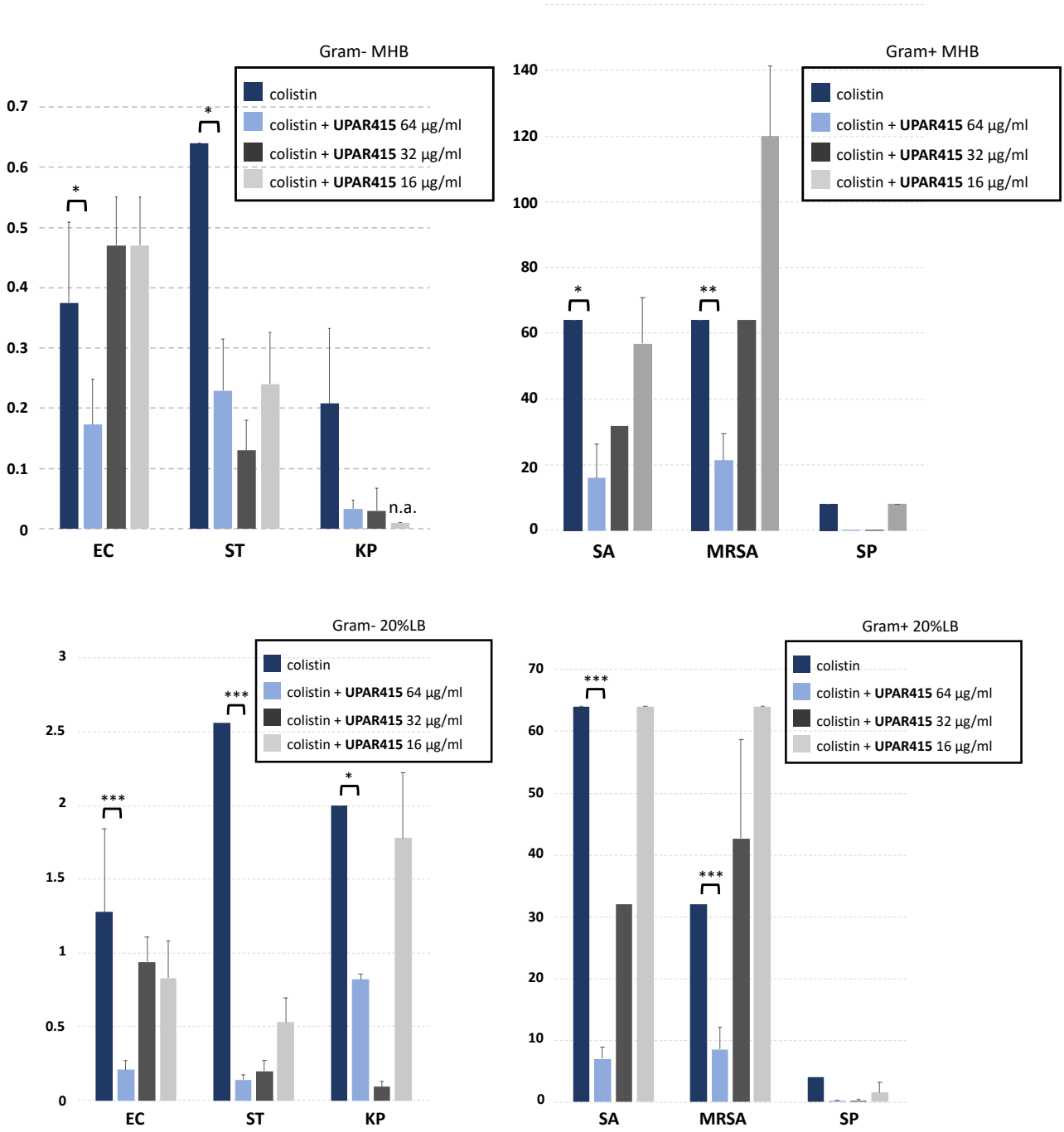

Figure 3. **Y Axis*:*** MIC (µg/ml) values of colistin alone or in combination with UPAR415 as an adjuvant, in Gram-negative and in Gram-positive bacteria, in both MHB and 20% LB broths. **X Axis**: Gram-negative and Gram-positive bacteria. Growth was assessed using optical density measurements at 540 nm and percent growth inhibition was calculated in comparison with cells incubated in a medium added with solvent alone (1% DMSO). The results are presented as the

average of three independent experiments, each carried out in triplicate, ± standard deviation (*p < 0.05, **p < 0.01, ***p < 0.001, between colistin alone and colistin + **UPAR415** 64 μg/ml, as determined by ANOVA).

The results of the growth of bacterial strains in 20% LB broth are similar to those in MHB (**Figure 3**). It is also possible to notice that the considered bacterial strains are more resistant to colistin effect in 20% LB medium and, especially in Gram-negative bacteria, the MIC value of colistin is higher than in MHB. These results are in agreement with the fact that the MIC for colistin is higher in 20% LB than in MHB for all Gram-negative bacteria tested, which might indicate that for these bacteria nutrient deprivation mimicks a stress condition, possibly similar to the one found under infection conditions that is often associated with an increased tendency to develop resitance. On the other hand, the MIC for colistin is higher all Gram-positive bacteria. In this case, it should be noted that colistin has a very limited potency on Gram-positive bacteria and produces a bactericidal effect only at high concentrations, both in 20% LB and MHB, when administered alone. The results in **Figure 3** show how, in Gram-positive bacteria, the MIC of colistin decreases when **UPAR415** is co-administered at 64 μg/ml.

These results are very promising for Gram-positive bacteria because they show that, using this combination, it is possible to widen the spectrum and the use of colistin reducing the dosage of such antibiotic.

Fractional Inhibitory Concentration (FIC) index determination

The Fractional Inhibitory Concentration (FIC) index is used to quantitatively determine the synergistic interaction between antibiotics and adjuvants. The FIC index method is one of the most accurate means for determining synergistic interactions when two inhibitors are studied in various combinations. A synergistic effect is assumed when the FIC index value of the compound of interest is ≤ 0.5. Previous research has also shown that the ratio in which an antibiotic and its adjuvant are

combined could influence the type of their interaction.[42] In **Table 2** is it possible to see the FIC index of the most potent combinations of **UPAR415** and colistin, both in MHB and 20% LB broths. Regarding the Gram-negative bacteria, the FIC index is consistently lower than or equal to 0.5, a value that indicates a syngergic interaction, except for of *E. coli*, for which the FIC index indicates an additive activity. Of notice, the FIC index is smaller when calculated for combinations in 20% LB, which indicates a more pronounced synergism. Regarding Gram-positive bacteria, the results indicate an additive activity for all the evaluated strains. These observations suggest that using an inhibitor of the cysteine biosynthetic pathway as an adjuvant in combination with colistin is a promising strategy to fight AMR.

Bacterial strains		**MHB**		**20% LB**	
	UPAR415 (μg/ml)	MIC colistin (μg/ml)	FIC Index	MIC colistin (μg/ml)	FIC Index
E. coli	64	0.17 ± 0.07	0.56 (Additivity)	0.21 ± 0.06	0.28 (Synergy)
S. T*yphimurium*	64	0.23 ± 0.08	0.48 (Synergy)	0.14 ± 0.01	0.17 (Synergy)
K. pneumoniae	64	0.03 ± 0.01	0.26 (Synergy)	0.08 ± 0.04	0.16 (Synergy)
S. aureus	64	16.00 ± 10.45	0.75 (Additivity)	7.00 ± 1.85	0.61 (Additivity)
MRSA	64	2133 ± 8.00	0.58 (Additivity)	8.57 ± 3.60	0.52 (Additivity)
S. pseudintermedius	64	0.23 ± 0.04	0.58 (Additivity)	0.23 ± 0.04	0.62 (Additivity)

Table 2. FIC index of the most potent combinations of **UPAR415** with colistin.

St CysK and CysM profiling and comparison with UPAR415 chemical inhibition

To establish the target engagement inside the bacterial cell of **UPAR415** and to prove that the phenotypic observation is linked to the chemical inhibition of OASS-A and/or OASS-B, target engagement experiments were performed. The DW378 mutant strain of *S.* Typhimurium, in which OASS-A and OASS-B were inactivated[43] , was used to demonstrate that administration of **UPAR415** leads to phenotypic manifestations matching those observed in the wild type bacterium. We measured the MIC of both **UPAR415** and colistin on the DW378 strain, to be compared with the values obtained on the WT strain. The effect on the MIC for colistin of the combination with 64 μg/ml **UPAR415** in the DW378 strain was also measured (**Table 3**).

Bacterial strain	**MIC UPAR415 (μg/ml)**	**MIC Colistin (μg/ml)**	**UPAR415 (μg/ml)**	**MIC Colistin (μg/ml)**
***S*. Typhimurium ATCC14028**	>256	0.71 ± 0.21	64	0.23 ± 0.08
***S*. Typhimurium DW378**	>256	0.14 ± 0.09	-	0.14 ± 0.09
			64	0.14 ± 0.07

Table 3. **UPAR415** tested in combination with colistin in *S.* Typhimurium wild type and mutant strains.

UPAR415 alone does not exert any bactericidal effect on the *Salmonella* DW378 strain, as observed for the WT strain. On the other hand, when the MIC assay was performed on the mutant strain, the MIC value of colistin was 5-fold lower than for the wild-type strain, a result in line with those obtained with the association of colistin and **UPAR415** in WT cells. To demonstrate that the synergistic effect is due only to the combined action of **UPAR415** and colistin in cells, a MIC assay

was performed using **UPAR415** at 64 µg/ml in combination with different concentrations of colistin in the DW378 strain. It is worth to notice that there is no change in colistin MIC in the presence of **UPAR415** in the OASS-inactivated strain. To further support the mechanism of action of **UPAR415** similar experiments were performed in M9 minimal media, deprived of relevant metabolites, including cysteine. The results are reported in Table 4 , showing that **UPAR415** alone again does not show any antibacterial activity, while colistin alone has a MIC of 16 ug/ml, which is significantly reduced by 64-fold when **UPAR415** is co-administered . Noteworthy, the synergistic effect of **UPAR415** is slightly counteracted when a 0.02 mM Cys replenishment is provided[44].

These results are in line with the hypothesis that the effect on bacterial cell viability is mainly due to the synergy of action between colistin and OASS inhibition.

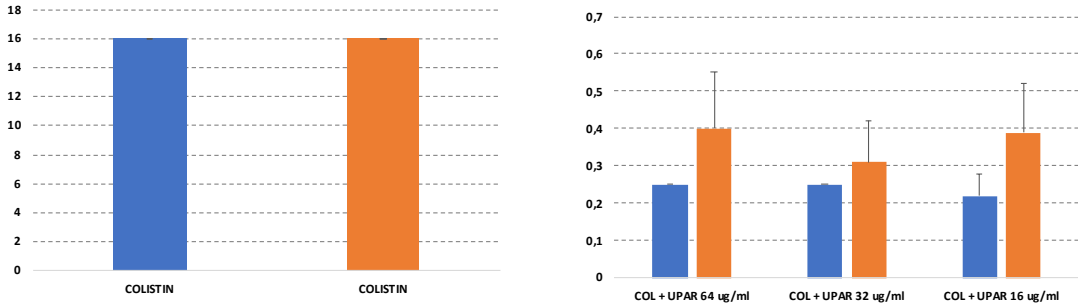

Figure 4. *Left:* **Y Axis*:*** MIC (µg/ml) values of colistin in *S.* Thyphymurium, in M9 (blue) and in M9 + 0.02 mM cysteine (orange) broths. *Right:* **Y Axis:** MIC (µg/ml) values of colistin for *S.* Thyphymurium, in M9 (blue) and in M9 + 0.02 mM cysteine (orange) broths. **X Axis**: association of colistin with different concentrations of **UPAR415**. Growth was assessed using optical density measurements at 540 nm and percent growth inhibition was calculated in comparison with cells incubated in a medium added with solvent alone (1% DMSO). The results are presented as the average of three independent experiments, each carried out in triplicate, ± standard deviation

Evaluation of UPAR415 toxicity

To evaluate the toxicity against eukaryotic cell membrane, the effect of **UPAR415** and **UPAR415**/colistin combination was evaluated at different concentrations for their ability to exert haemolytic activity against sheep defibrinated blood cells. Moreover we evaluated the toxicity of

the combination also as the viability of cells derived from a kidney of a normal adult bovine (MDBK) growing *in-vitro* after the treatment of colistin/UPAR415 or UPAR415 alone. The results demonstrated that after 16 hours of incubation, negligible haemolytic activity (<1%) was observed in control wells, as well as at 24 hours (Table 5). Very low haemolytic activity compared with controls (not greater than 2%) was observed at 32 and 64 while at 256 µg/ml it was around 5%. Also in MDBK cell lines **UPAR415** did not show toxicity (Figure 5), indicating a safe profile of either the compound alone or in association with colistin. Hemolytic activity was only detectable when a high colistin concetration (256 ug/ml) has been used, likely highlighting safety issues linked to colistin. Such colistin concentration is significantly higher than the concentration required to exert the synergistic effect (Table 5 *vs*. Table 2), supporting the notion that the **UPAR415**/colistin combination has no toxic effect on eukaryotic cells.

UPAR415/Association	**% Emolysis**	**% Viability of MDBK cells**
UPAR415 16 µg/ml	0.255%	71.76 ± 9.78%
UPAR415 16 µg/ml + colistin 0.125 µg/ml	0.151%	74.85 ± 10.39%
UPAR415 16 µg/ml + colistin 256 µg/ml	0.288%	67.13 ± 16.82%
UPAR415 32 µg/ml	0.514%	85.97 ± 6.88%
UPAR415 32 µg/ml + colistin 0.125 µg/ml	0.442%	81.74 ± 9.80%
UPAR415 32 µg/ml + colistin 256 µg/ml	0.546%	66.86 ± 11.87%
UPAR415 64 µg/ml	1.206%	80.14 ± 9,68%
UPAR415 64 µg/ml + colistin 0.125 µg/ml	0.837%	91.53 ± 12.50%
UPAR415 64 µg/ml + colistin 256 µg/ml	0.748%	73.52 ± 7.24%
UPAR415 256 µg/ml	5.07%	93.67 ± 9.75%
colistin 0.125 µg/ml	-	87.99 ± 7.29%
colistin 256 µg/ml	-	52.95 ± 16.77%
PC + DMSO 1%	-	117 ± 18.38%
PC	100%	100%

Table 5. Evaluation of the toxicity of **UPAR415** alone and in association with colistin as haemolytic activity and as viability of MDBK cells growing *in-vitro*. Growth was assessed using optical density measurements at 620 nm and percent growth inhibition was calculated in comparison with cells incubated in a medium added with solvent alone (1% DMSO). The results are presented as the average of three independent experiments, each carried out in triplicate, ± standard deviation. PC means positive control.

Structure of UPAR415 in complex with OASS

The promising results obtained in microbiology with **UPAR415** encouraged further investigations to understand the molecular details of the interaction of the inhibitor with the enzyme. To confirm the functional data suggesting a competitive binding mechanism with respect to the first substrate of the enzyme, OAS,[16] the crystal structure of *Salmonella* OASS-A was determined in complex with **UPAR415** at 1.2 Å resolution. Notably, the only available structure of OASS-A from *Salmonella* complexed with a small organic molecule was obtained in 1999 when a purification-derived methionine was found bound in the active site of a K41A mutant (PDB id: 1D6S).[45] The structure of OASS-A from *Salmonella* was also determined in the unligated form (PDB id: 1OAS) [46] and in the inhibited form; the latter had a sulphate bound in the active site and a chloride ion bound in an allosteric site (PDB code: 1FCJ).[47] In a structure of *Haemophilus influenzae* OASS-A in complex with a decapeptide that mimics the C-terminus of SAT (PDB code: 1Y7L),[24] only the four C-terminal amino acids (NLNI) where visible while the rest of the sequence was disordered. This structure was originally used as a starting point for the design of peptidic[16,19,48] and non-peptidic inhibitors of OASS that led to the identification of **UPAR415**.[15] Using a modification of the crystallization protocol by Burkhard[46] we obtained well-diffracting crystals of OASS-A bound to **UPAR415**. Crystals belonged to the space group $P2_12_12_1$ with unit cell parameters a = 56.67 Å, b = 122.87 Å, c = 127.52 Å, α=β=γ=90° and contained one dimer per asymmetric unit. Detailed data collection statistics are shown in **Table 4**. The three-dimensional structure of the dimer is represented in **Figure 5, panel A**. The overall final model contains a well-defined electron density for the entire main chain of each polypeptide in the dimer, except for the last C-terminal residues. The protein adopts the fold of a type II pyridoxal 5'-phosphate (PLP)-dependent enzyme with each protomer having the PLP cofactor

linked as an internal aldimine to Lys41 (residues are numbered as in 1OAS). No significant differences are observed among the dimer chains, that superimpose well with rmsd of 0.12 (aligned in Pymol).

UPAR415 density was clearly identified near the PLP cofactor (**Figure 5, panel B**), with the two aromatic substituents on the cyclopropane ring pointing towards the active site entrance (**Figure 5, panel A**) and forming hydrophobic interactions with residues lining the pocket (Phe143, Ile229, Ala231, **Figure 5, panel C**). The carboxylate group of **UPAR415** forms hydrogen bonds with the side chains of Thr68, Thr72 and Glu142, with the main chains of Asp71 and Thr72, and with a water molecule, and inserts deeply into the active site occupying a position close to the one occupied by the carboxylate group of methionine in the 1D6S structure (**Figure 5, panel D**).

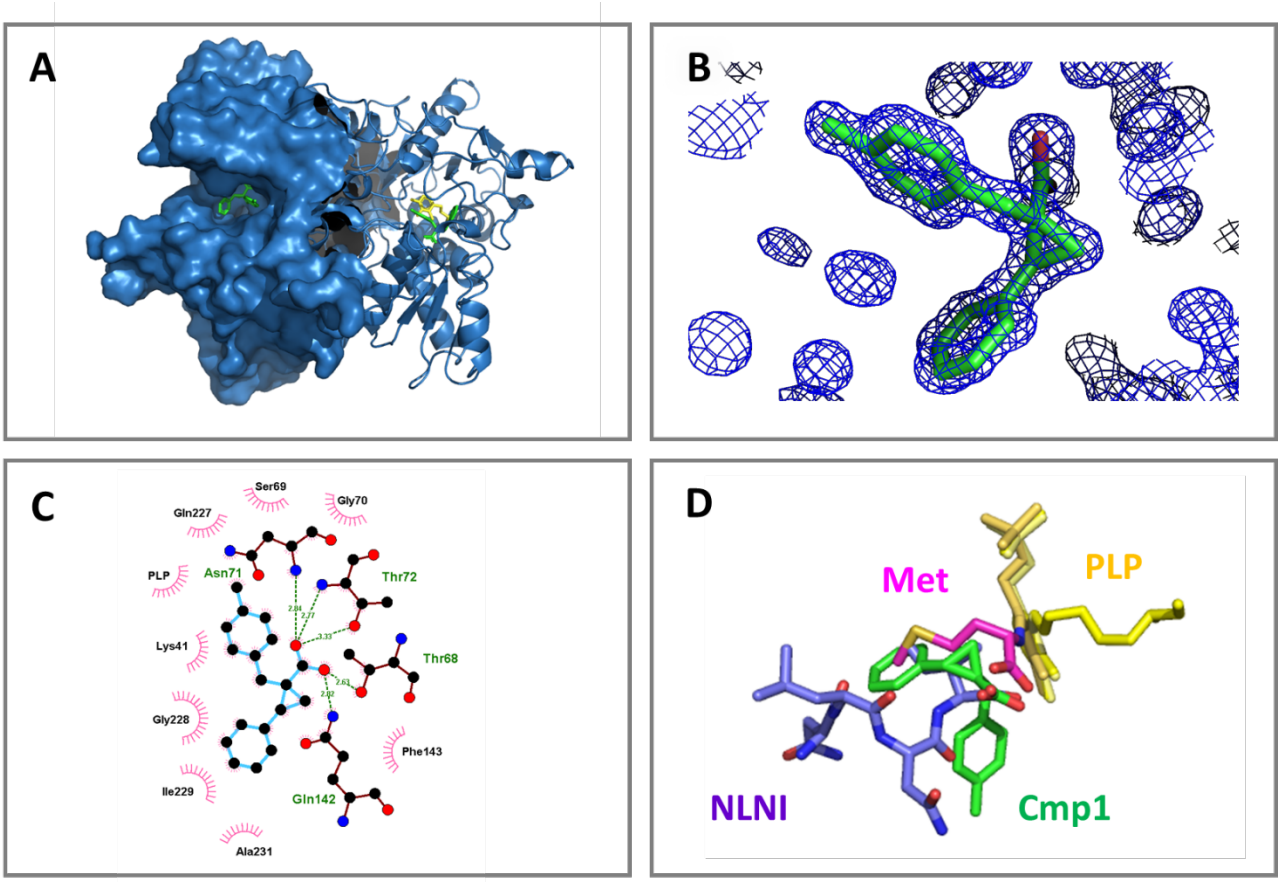

Figure 5. Three-dimensional structure of the complex between OASS-A and UPAR415. **Panel A**: OASS-A dimer is represented, with one monomer shown in ribbon and one monomer shown in surface mode. The PLP cofactor is shown in yellow and **UPAR415** in green. Both ligands are shown in stick mode. **Panel B:** UPAR415 modeled inside the electron density is represented in stick mode. **Panel C:** LigPlot showing the residues involved in the interaction with UPAR415 in the active site of OASS-A. **Panel D:** superposition of 6Z4N (PDB code of this entry) with 1D6S and 1Y7L. The protein structure has been removed from the representation and only PLP and ligands are shown. Ligands are as follows: Met

(pink) bound as an external aldimine to PLP (from 1D6S); NLNI tetrapeptide (purple) (from 1Y7L); UPAR415 (Cmp1, green) (from 6Z4N).

Even more relevant is the almost perfect overlap between the carboxylate group of **UPAR415** and the C-terminal carboxylate of the NLNI peptide (**Figure 5, panel D**). The observation that the carboxylate of **UPAR415** occupies the same position of the carboxylate group of both peptidic and non-peptidic ligands of the protein suggests that it should bind to the same carboxylate subsite of the active site that was identified as essential for anchoring the ligand to the enzyme.[45] This subsite was identified for the complex between OASS-A and methionine (1D6S) and its occupation is considered key for triggering a movement of the so-called asparagine loop (also known as substrate-binding loop, SB loop) that pulls a whole subdomain of the N-terminal domain of the protein, thus leading to the closure of the active site entrance. In the presence of methionine the stable structure of OASS-A is indeed a closed state, where the N-terminal subdomain has undergone a rotation moving by 7 Å towards the active site entrance. On the other hand, the structure in the presence of NLNI peptide is in the open form, demonstrating that, in this case, ligand binding does not trigger active site closure. We thus superimposed the **UPAR415**/OASS-A structure with the open (1OAS), intermediate/inhibited (1FCJ) and closed (1D6S), structures in their dimeric form. The structural alignments resulted in rmsd of 0.576, 0.607, and 1.081 for open intermediate and closed structures, respectively. The superpositions are shown in **Figure 6**.

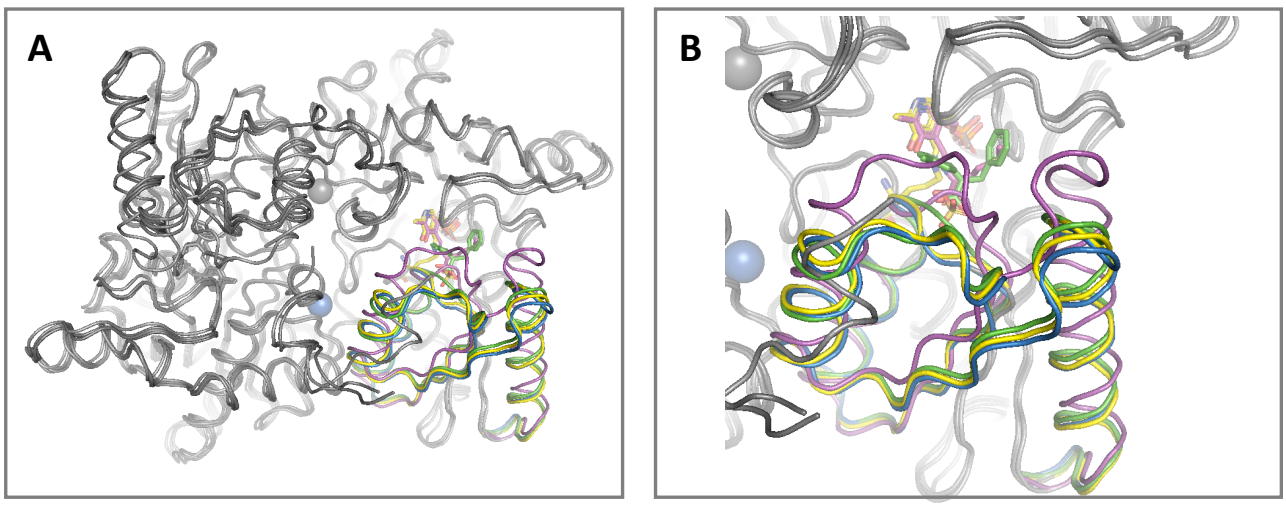

Figure 6. **Superposition of the the open, inhibited and closed structures of OASS-A in complex with UPAR415**. Panel A: structural alignement of the UPAR415 inhibited OASS-A (6Z4N, green) to the open unligated form (1OAS, yellow), to the intermediate-allosterically inhibited form (1FCJ, blue), and to the closed-methionine bound form (1D6S, magenta). The relative cofactor and ligands are represented as stick and bond, while the Cl^- ions are as blue spheres. Panel B: close-up view of the binding site region, where the movement of helix 3-SB loop-helix 4 is visible.

Based on this analysis **UPAR415** is able to induce only a partial closure of the active site, and thus locks the enzyme in an almost open conformation resembling the 1OAS unligated structure as well as that of the allosterically inhibited structure of 1FCJ. We further explored this feature and compared the position of the SB loop and nearby regions in the present and in the closed structure (**Figure 7**). The SB loop moves toward the cofactor in the closed structure and contributes to the narrowing of the active site. This large movement is not triggered by **UPAR415**, probably because the loop would clearly clash with the tolyl substituent of the cyclopropane in the closed conformation. Notably, the electron density for some residues belonging to the SB loop and helix 4 can be fitted to two alternative conformations, with about 50% occupancy each, suggesting that this strech of the sequence is not stabilized by the ligand in a defined conformation.

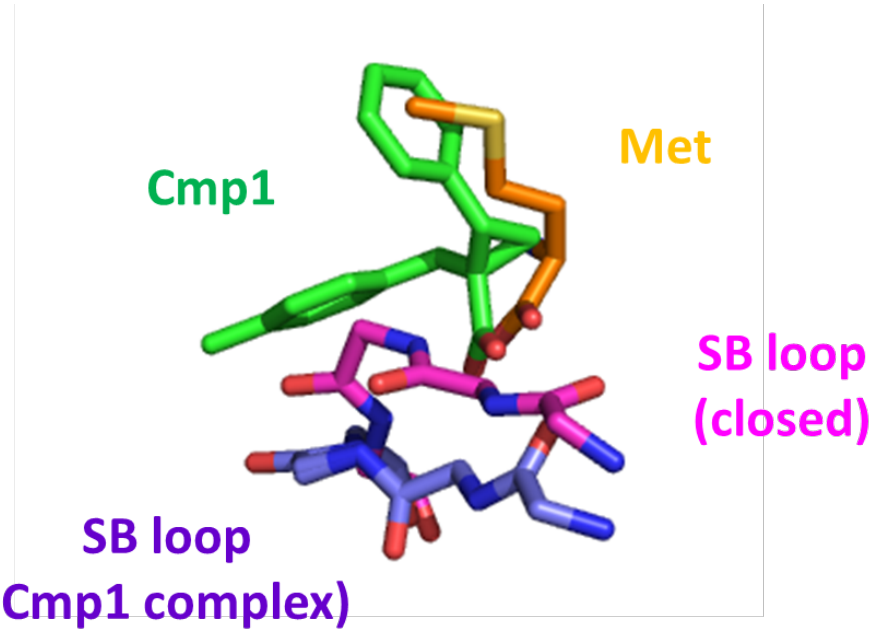

Figure 7. Detail of the superposition of the structure of OASS-A in complex with **UPAR415** with the closed structure of OASS-A in complex with methionine.

Conclusions

UPAR415 was tested as an adjuvant in combination with colistin at different concentrations, revealing a synergistic or additive effect against all the bacterial species considered in this study. Moreover, the use of *S.* Typhimurium DW378 strain, in which the genes encoding for OASS-A and OASS-B were inactivated, revealed that the phenotypic effect due to chemical inhibition of the enzymes is overlapping the phenotypic effects observed in the *cysK* and *cysM* inactivated *S.* Typhimurium strain, supporting the notion that **UPAR415** acts in the cell by inhibiting both OASS-A and -B isoforms. The specific mechanism by which UPAR415 exherts its synergy with colistin is still to be determined. It can be speculated, however, that while at sub-MIC concentration, colistin starts stressing the bacteria which respond to the stressful event by activating cytoplasmatic pathways. If these pathways -including the cysteine biosynthetic pathway– are inhibited, then the antibiotic activity of colistin appear to be evident at lower concentration.

UPAR415 resulted to be non-toxic in haemolysis tests, highlighting that such compound does not disrupt biological membranes.

Finally, the 3D structure of **UPAR415** in complex with OASS-A was resolved by X-ray diffraction studies confirming that the ligand binds in the active site and competes with the amino acidic substrate. Furthermore, the ligand is able to elicit only a modest closure of the active site, likely as a consequence of steric clashes between the tolyl substituent and the SB loop in the completely closed conformation. This result is very relevant for the design of better ligands of OASS and will pave the way for further cycles of medicinal chemistry optimization in the context of the multiparametric optimization process.

Our results suggest that it is possible to identify compounds able to selectively target the microbial reductive sulfur assimilation pathway by interfering with both OASS isoforms, providing a good

starting point supporting OASS as potential pharmaceutical target to develop a new class of antimicrobial adjuvants.

EXPERIMENTAL SECTION

MIC test

MIC values were evaluated following the CLSI guidelines with some modifications (CLSI, 2018b).[49] Reference bacterial strains were inoculated in sterile Müller Hinton Broth (MHB) and incubated overnight at 37 °C. The bacterial suspension was centrifuged 20 min at 2000 rpm and 4 °C, then the pellet was resuspended in phosphate buffer. The turbidity of the bacterial suspension was immediately measured and adjusted by spectrophotometry. At 600 nm, the OD range 0.08-0.13 was considered to correspond to a bacterial concentration of 10^8 CFU/ml. The obtained suspension was further diluted 1:100 in appropriate medium to obtain a final bacterial concentration of 10^6 CFU/ml, and inoculated within 30 min.

MIC assay was performed in 96 wells microtiter plates by incubating colistin at concentrations ranging from 256 μg/ml to 0.5 μg/ml with a final concentration of $5x10^5$ CFU/ml of bacterial suspension in a volume of 100 μl. Growth and sterility controls were performed.

For each test, three independent experiments, with three replicates each, were performed.

After 24 hours of incubation, MIC value was evaluated as the arithmetic average of the lowest concentration of colistin that completely inhibited the bacterial growth as detected by the unaided eye. Standard deviation from average MIC value was also calculated. Quality control organism (*E. coli* ATCC 25922) was tested periodically to validate the accuracy of the procedure.

OD plate readings were performed at 620 nm.

Checkerboard assay

Associations between colistin as antibiotic and UPAR415 as adjuvant were evaluated by checkerboard assay.

96 wells microtiter plates were prepared with serial dilutions of colistin in MHB from MIC concentration with 10 twofold dilutions, in order to have the final concentration in 100 µl. In each well of the same replicate 1 µl of UPAR415 in DMSO has been added, at a fixed concentration 100 times higher than the final concentration desired. Plates were finally incubated with a bacterial suspension of $5x10^5$ CFU/ml, adjusted spectrophotometrically as reported above.

Each plate was incubated overnight at 37 °C in aerobic atmosphere.

To evaluate the antimicrobial effect of two molecules in association, the Fractional Inhibitory Concentration (FIC) index was calculated [40]. MIC of each of the two molecules tested individually and in combination with each other was evalued. The results have been included in the following formula:

$$FIC = \frac{MIC_{A\ in\ combination}}{MIC_A} + \frac{MIC_{B\ in\ combination}}{MIC_B}$$

On the basis of the FIC index value, the antimicrobial activity of the associations could be synergistic, additive, indifferent or antagonistic. In particular the molecules are synergic if FIC is ≤ 0.5; additive if FIC is included between 0.5 and 1; indifferent if FIC is included between 1 and 4; antagonist if FIC is > 4.

Hemolysis assay

Sheep defibrinated blood was purchased from Thermofisher Diagnostics, lot n. 36889400.

In a U bottomed 96 wells sterile plate 50 µl of sheep defibrinated blood were incubated with 49 µl of sterile saline and 1 µl of UPAR415 at variable concentrations for 24 hours at room temperature. Positive (100% haemoglobin release) and negative (0% haemoglobin release) controls were respectively set up with sterile water and sterile saline added to 1% of sterile DMSO. After incubation, the test plate was centrifuged at 1400 rpm for 15 min and, after transferring the supernatant in a sterile plate, haemolysis was measured at 450 nm. Haemolysis percentage was calculated as follows:

$$\left[1 - (A_{comp} - A_{NC}) / (A_{PC} - A_{NC})\right] x\ 100$$

where A_{comp} represents the optical density of the samples at 450 nm, A_{PC} the optical density of the positive control and A_{NC} the optical density of the negative control.

Citotoxicity on MDBK cells assay

One microliter of UPAR 415 in DMSO at different concentrations was added in each well of 96-wells plates containing 100 µl of MDBK cells in DMEM medium. Plates were incubated for 24 hours at 37 °C in the presence of 5% CO_2. After incubation, 10 µl of MTT (3-(4,5-dimethylthiazol-2-yl)-2,5diphenyltetrazolium bromide) were added to each well and incubated at 37 °C for 6 hours. At the end of the incubation, 100 µl of the solubilization solution (10% SDS in 0.01 M HCl) were added to each well and then incubated overnight. The yellow tetrazolium MTT salt is reduced in metabolically active cells to form insoluble purple formazan crystals, which are solubilized by the addition of a detergent. After incubation plates were read with a spectrophotometer (620 nm). Positive and negative controls were performed for each plate.[50] Three replicates for two independent experiments were performed for each assay.

Antibiotics:

Colistin was purchased from Sigma-Aldrich, MO, USA, lot n. 049M-4836V.

All the stock solutions were stored in small aliquots at – 80 °C until use.

Bacterial strains:

The following reference strains were tested:

Salmonella enterica subsp. *enterica* serovar Typhimurium ATCC 14028,

Staphylococcus aureus ATCC 25923,

Methicillin-resistant *Staphylococcus aureus* (MRSA) ATCC 43300,

Escherichia coli ATCC 25922,

Klebsiella pneumoniae ATCC13883,

Staphylococcus pseudintermedius ATCC21284

The *Salmonella* Typhimurium DW378 strain defective for OASS-A and OASS-B (genotype: trpC109, cysK1772, cysM1770) was used to confirm target engagement. DW378 is auxotroph for cysteine and L-tryptophan and azaserine-resistant[43]. The strain was identified in a study aimed at the isolation of strains lacking OASS-B in the genetic background of the TK181 strain lacking OASS-A. In the original paper the DW378 strain is reported to completely lack *O*-acetylserine sulfhydyrlase activity, but no ultimate proof of the molecular origin of this phenotype is given. We demonstrate that OASS-A is expressed at comparable amounts in the wild-type and DW378 strains, whereas OASS-B expression is undetectable both in the wild type and in the DW378 strains (Supplemental Material and Figure S1). Therefore, cysteine auxotrophy is due to inactivation of the enzyme but not to complete deletion of the coding gene.

UPAR415

UPAR415 has been synthesized and characterized as reported by Pieroni et al.[15]

UPAR415 was dissolved in DMSO to a stock solution of 25.6 mg/ml, then tested at a final concentration comprised in the range of 256-0.5 µg/ml, containing a maximum of 1% DMSO.

Crystallization and data collection

Crystallization and data collection

OASS-A was produced from *E. coli* expression and purified as described in Franko et al.[12] Crystallization was performed by hanging drop vapor diffusion at similar conditions as described in Burkhard et al.[46] Drops contained 1 µL of 20 mg/mL StOASS-A mixed with 1 µL of reservoir solution containing 30-31% PEG4000 (w/v), 130 – 180 mM Li_2SO_4 (Fluka), 100 mM Tris base pH 7.0. Crystals grew within 5 days at 25 °C as monoclinic plates of 1.1 mm x 0.4 mm x 0.1 mm dimension. The crystals were soaked for 2 hours at RT in a solution containing 1 mM UPAR415, 32% PEG 4000 (w/v), 150 mM $LiSO_4$, 100 mM Tris pH 7.0 and 5% glycerol (as cryoprotectant agent) and subsequently flash frozen in liquid nitrogen to be measured.

Diffraction data were collected at the Elettra XRD1 beamline (Trieste, Italy) using Pilatus 6M (Dectris) detector and processed by XDS program.[51]

Structure determination and refinement

The structure was solved by molecular replacement direct fft using the structure of (PDB code 1OAS) by rigid body procedure, implemented in PHASER of the CCP4 software suite.[52] Flexible loops of the protein, PLP cofactor and water molecules were removed from the initial model to exclude model bias during the first round of refinement. The UPAR415 molecule [DRG] manually fitted in the FoFc electron density map. The model was improved using manual rebuilding with COOT[53] and maximum likelihood refinement using REFMAC5.[54] The final step of the structure refinement was performed to 1.2 Å with R_{work} of 15.9% and R_{free} of 18.2% (Table 4). Structural alignments were calculated using

GESAMT algorithm[55], structure analyses were performed using COOT and PyMOL(TM) 2.0.6, Schrodinger, LLC (The PyMOL Molecular Graphics System, Version 2.0 Schrödinger, LLC.)

The structure has been submitted to the Protein Data Bank with PDB code 6Z4N.

	OASS-UPAR415
Wavelength	1
Resolution range	46.6 - 1.2 (1.243 - 1.2)
Space group	*P* 2_1 2_1 2_1
Unit cell	53.261 96.275 140.835 90 90 90
Total reflections	409172 (22602)
Unique reflections	214538 (14933)
Multiplicity	1.9 (1.5)
Completeness (%)	94.35 (65.85)
Mean I/sigma(I)	10.89 (0.72)
Wilson B-factor	10.08
R-merge	0.0286 (0.5601)
R-meas	0.04044 (0.7921)
R-pim	0.0286 (0.5601)
CC1/2	0.999 (0.569)
CC*	1 (0.852)
Reflections used in refinement	213161 (14736)
Reflections used for R-free	10571 (747)
R-work	0.1596 (0.2977)

R-free	0.1824 (0.3058)
CC(work)	0.942 (0.402)
CC(free)	0.918 (0.466)
Number of non-hydrogen atoms	6208
macromolecules	5156
ligands	103
solvent	949
Protein residues	639
RMS(bonds)	0.016
RMS(angles)	1.95
Ramachandran favored (%)	97.48
Ramachandran allowed (%)	2.52
Ramachandran outliers (%)	0.00
Rotamer outliers (%)	1.40
Clashscore	10.02
Average B-factor	17.90
macromolecules	16.91
ligands	18.19
solvent	23.22

Table 6. Data collection and refinement statistics. Values in parentheses are for the highest resolution shell. $CC_{1/2}$ is the Pearson's correlation coefficient calculated for I_{mean} by splitting the data randomly in half by AIMLESS/SCALA.[56] Statistics for the highest-resolution shell are shown in parentheses.

REFERENCES

(1) Davies, J.; Davies, D. Origins and Evolution of Antibiotic Resistance. *Microbiol. Mol. Biol.*

Rev. **2010**, *74* (3), 417–433. https://doi.org/10.1128/MMBR.00016-10.
(2) Fair, R. J.; Tor, Y. Antibiotics and Bacterial Resistance in the 21st Century. *Perspect. Med. Chem.* **2014**, *6*, PMC.S14459. https://doi.org/10.4137/PMC.S14459.
(3) Aslam, B.; Wang, W.; Arshad, M. I.; Khurshid, M.; Muzammil, S.; Rasool, M. H.; Nisar, M. A.; Alvi, R. F.; Aslam, M. A.; Qamar, M. U.; Salamat, M. K. F.; Baloch, Z. Antibiotic Resistance: A Rundown of a Global Crisis. *Infect. Drug Resist.* **2018**, *Volume 11*, 1645–1658. https://doi.org/10.2147/IDR.S173867.
(4) González-Bello, C. Antibiotic Adjuvants – A Strategy to Unlock Bacterial Resistance to Antibiotics. *Bioorg. Med. Chem. Lett.* **2017**, *27* (18), 4221–4228. https://doi.org/10.1016/j.bmcl.2017.08.027.
(5) Annunziato. Strategies to Overcome Antimicrobial Resistance (AMR) Making Use of Non-Essential Target Inhibitors: A Review. *Int. J. Mol. Sci.* **2019**, *20* (23), 5844. https://doi.org/10.3390/ijms20235844.
(6) Rogers, G. B.; Carroll, M. P.; Bruce, K. D. Enhancing the Utility of Existing Antibiotics by Targeting Bacterial Behaviour?: Enhancing Antibiotics Utility. *Br. J. Pharmacol.* **2012**, *165* (4), 845–857. https://doi.org/10.1111/j.1476-5381.2011.01643.x.
(7) Darrell, J. H.; Garrod, L. P.; Waterworth, P. M. Trimethoprim: Laboratory and Clinical Studies. *J. Clin. Pathol.* **1968**, *21* (2), 202–209. https://doi.org/10.1136/jcp.21.2.202.
(8) Clatworthy, A. E.; Pierson, E.; Hung, D. T. Targeting Virulence: A New Paradigm for Antimicrobial Therapy. *Nat. Chem. Biol.* **2007**, *3* (9), 541–548. https://doi.org/10.1038/nchembio.2007.24.
(9) Garland, M.; Loscher, S.; Bogyo, M. Chemical Strategies To Target Bacterial Virulence. *Chem. Rev.* **2017**, *117* (5), 4422–4461. https://doi.org/10.1021/acs.chemrev.6b00676.
(10) Petchiappan, A.; Chatterji, D. Antibiotic Resistance: Current Perspectives. *ACS Omega* **2017**, *2* (10), 7400–7409. https://doi.org/10.1021/acsomega.7b01368.
(11) Campanini, B.; Pieroni, M.; Raboni, S.; Bettati, S.; Benoni, R.; Pecchini, C.; Costantino, G.; Mozzarelli, A. Inhibitors of the Sulfur Assimilation Pathway in Bacterial Pathogens as Enhancers of Antibiotic Therapy. *Curr. Med. Chem.* **2014**, *22* (2), 187–213. https://doi.org/10.2174/0929867321666141112122553.
(12) Franko, N.; Grammatoglou, K.; Campanini, B.; Costantino, G.; Jirgensons, A.; Mozzarelli, A. Inhibition of *O* -Acetylserine Sulfhydrylase by Fluoroalanine Derivatives. *J. Enzyme Inhib. Med. Chem.* **2018**, *33* (1), 1343–1351. https://doi.org/10.1080/14756366.2018.1504040.
(13) Magalhães, J.; Franko, N.; Annunziato, G.; Pieroni, M.; Benoni, R.; Nikitjuka, A.; Mozzarelli, A.; Bettati, S.; Karawajczyk, A.; Jirgensons, A.; Campanini, B.; Costantino, G. Refining the Structure−activity Relationships of 2-Phenylcyclopropane Carboxylic Acids as Inhibitors of O-Acetylserine Sulfhydrylase Isoforms. *J. Enzyme Inhib. Med. Chem.* **2019**, *34* (1), 31–43. https://doi.org/10.1080/14756366.2018.1518959.
(14) Magalhães, J.; Franko, N.; Annunziato, G.; Welch, M.; Dolan, S. K.; Bruno, A.; Mozzarelli, A.; Armao, S.; Jirgensons, A.; Pieroni, M.; Costantino, G.; Campanini, B. Discovery of Novel Fragments Inhibiting O-Acetylserine Sulphhydrylase by Combining Scaffold Hopping and Ligand–Based Drug Design. *J. Enzyme Inhib. Med. Chem.* **2018**, *33* (1), 1444–1452. https://doi.org/10.1080/14756366.2018.1512596.
(15) Pieroni, M.; Annunziato, G.; Beato, C.; Wouters, R.; Benoni, R.; Campanini, B.; Pertinhez, T. A.; Bettati, S.; Mozzarelli, A.; Costantino, G. Rational Design, Synthesis, and Preliminary Structure–Activity Relationships of α-Substituted-2-Phenylcyclopropane Carboxylic Acids as Inhibitors of Salmonella Typhimurium O-Acetylserine Sulfhydrylase. *J. Med. Chem.* **2016**, *59* (6), 2567–2578. https://doi.org/10.1021/acs.jmedchem.5b01775.
(16) Spyrakis, F.; Singh, R.; Cozzini, P.; Campanini, B.; Salsi, E.; Felici, P.; Raboni, S.; Benedetti, P.; Cruciani, G.; Kellogg, G. E.; Cook, P. F.; Mozzarelli, A. Isozyme-Specific Ligands for O-Acetylserine Sulfhydrylase, a Novel Antibiotic Target. *PLoS ONE* **2013**, *8* (10), e77558. https://doi.org/10.1371/journal.pone.0077558.

(17) Amori, L.; Katkevica, S.; Bruno, A.; Campanini, B.; Felici, P.; Mozzarelli, A.; Costantino, G. Design and Synthesis of Trans-2-Substituted-Cyclopropane-1-Carboxylic Acids as the First Non-Natural Small Molecule Inhibitors of O-Acetylserine Sulfhydrylase. *MedChemComm* **2012**, *3* (9), 1111. https://doi.org/10.1039/c2md20100c.
(18) Annunziato, G.; Pieroni, M.; Benoni, R.; Campanini, B.; Pertinhez, T. A.; Pecchini, C.; Bruno, A.; Magalhães, J.; Bettati, S.; Franko, N.; Mozzarelli, A.; Costantino, G. Cyclopropane-1,2-Dicarboxylic Acids as New Tools for the Biophysical Investigation of O-Acetylserine Sulfhydrylases by Fluorimetric Methods and Saturation Transfer Difference (STD) NMR. *J. Enzyme Inhib. Med. Chem.* **2016**, *31* (sup4), 78–87. https://doi.org/10.1080/14756366.2016.1218486.
(19) Salsi, E.; Bayden, A. S.; Spyrakis, F.; Amadasi, A.; Campanini, B.; Bettati, S.; Dodatko, T.; Cozzini, P.; Kellogg, G. E.; Cook, P. F.; Roderick, S. L.; Mozzarelli, A. Design of *O* -Acetylserine Sulfhydrylase Inhibitors by Mimicking Nature. *J. Med. Chem.* **2010**, *53* (1), 345–356. https://doi.org/10.1021/jm901325e.
(20) Brunner, K.; Maric, S.; Reshma, R. S.; Almqvist, H.; Seashore-Ludlow, B.; Gustavsson, A.-L.; Poyraz, Ö.; Yogeeswari, P.; Lundbäck, T.; Vallin, M.; Sriram, D.; Schnell, R.; Schneider, G. Inhibitors of the Cysteine Synthase CysM with Antibacterial Potency against Dormant *Mycobacterium Tuberculosis*. *J. Med. Chem.* **2016**, *59* (14), 6848–6859. https://doi.org/10.1021/acs.jmedchem.6b00674.
(21) Wallace, M. J.; Dharuman, S.; Fernando, D. M.; Reeve, S. M.; Gee, C. T.; Yao, J.; Griffith, E. C.; Phelps, G. A.; Wright, W. C.; Elmore, J. M.; Lee, R. B.; Chen, T.; Lee, R. E. Discovery and Characterization of the Antimetabolite Action of Thioacetamide-Linked 1,2,3-Triazoles as Disruptors of Cysteine Biosynthesis in Gram-Negative Bacteria. *ACS Infect. Dis.* **2020**, *6* (3), 467–478. https://doi.org/10.1021/acsinfecdis.9b00406.
(22) Campanini, B.; Benoni, R.; Bettati, S.; Beck, C. M.; Hayes, C. S.; Mozzarelli, A. Moonlighting O-Acetylserine Sulfhydrylase: New Functions for an Old Protein. *Biochim. Biophys. Acta BBA - Proteins Proteomics* **2015**, *1854* (9), 1184–1193. https://doi.org/10.1016/j.bbapap.2015.02.013.
(23) Townsend, D. M.; Tew, K. D.; Tapiero, H. Sulfur Containing Amino Acids and Human Disease. *Biomed. Pharmacother.* **2004**, *58* (1), 47–55. https://doi.org/10.1016/j.biopha.2003.11.005.
(24) Huang, B.; Vetting, M. W.; Roderick, S. L. The Active Site of O-Acetylserine Sulfhydrylase Is the Anchor Point for Bienzyme Complex Formation with Serine Acetyltransferase. *J. Bacteriol.* **2005**, *187* (9), 3201–3205. https://doi.org/10.1128/JB.187.9.3201-3205.2005.
(25) Rosa, B.; Marchetti, M.; Paredi, G.; Amenitsch, H.; Franko, N.; Benoni, R.; Giabbai, B.; De Marino, M. G.; Mozzarelli, A.; Ronda, L.; Storici, P.; Campanini, B.; Bettati, S. Combination of SAXS and Protein Painting Discloses the Three-Dimensional Organization of the Bacterial Cysteine Synthase Complex, a Potential Target for Enhancers of Antibiotic Action. *Int. J. Mol. Sci.* **2019**, *20* (20), 5219. https://doi.org/10.3390/ijms20205219.
(26) Benoni, R.; De Bei, O.; Paredi, G.; Hayes, C. S.; Franko, N.; Mozzarelli, A.; Bettati, S.; Campanini, B. Modulation of *Escherichia Coli* Serine Acetyltransferase Catalytic Activity in the Cysteine Synthase Complex. *FEBS Lett.* **2017**, *591* (9), 1212–1224. https://doi.org/10.1002/1873-3468.12630.
(27) Mozzarelli, A.; Bettati, S.; Campanini, B.; Salsi, E.; Raboni, S.; Singh, R.; Spyrakis, F.; Kumar, V. P.; Cook, P. F. The Multifaceted Pyridoxal 5′-Phosphate-Dependent O-Acetylserine Sulfhydrylase. *Biochim. Biophys. Acta BBA - Proteins Proteomics* **2011**, *1814* (11), 1497–1510. https://doi.org/10.1016/j.bbapap.2011.04.011.
(28) Amori, L.; Katkevica, S.; Bruno, A.; Campanini, B.; Felici, P.; Mozzarelli, A.; Costantino, G. Design and Synthesis of Trans-2-Substituted-Cyclopropane-1-Carboxylic Acids as the First Non-Natural Small Molecule Inhibitors of O-Acetylserine Sulfhydrylase. *MedChemComm* **2012**, *3* (9), 1111. https://doi.org/10.1039/c2md20100c.
(29) Turnbull, A. L.; Surette, M. G. L-Cysteine Is Required for Induced Antibiotic Resistance in

Actively Swarming Salmonella Enterica Serovar Typhimurium. *Microbiology* **2008**, *154* (11), 3410–3419. https://doi.org/10.1099/mic.0.2008/020347-0.
(30) Karaiskos, I.; Lagou, S.; Pontikis, K.; Rapti, V.; Poulakou, G. The "Old" and the "New" Antibiotics for MDR Gram-Negative Pathogens: For Whom, When, and How. *Front. Public Health* **2019**, *7*, 151. https://doi.org/10.3389/fpubh.2019.00151.
(31) Oka, H.; Ito, Y. ANTIBIOTICS | High-Speed Countercurrent Chromatography. In *Encyclopedia of Separation Science*; Elsevier, 2000; pp 2058–2067. https://doi.org/10.1016/B0-12-226770-2/03311-1.
(32) Dupuy, F. G.; Pagano, I.; Andenoro, K.; Peralta, M. F.; Elhady, Y.; Heinrich, F.; Tristram-Nagle, S. Selective Interaction of Colistin with Lipid Model Membranes. *Biophys. J.* **2018**, *114* (4), 919–928. https://doi.org/10.1016/j.bpj.2017.12.027.
(33) Biswas, S.; Brunel, J.-M.; Dubus, J.-C.; Reynaud-Gaubert, M.; Rolain, J.-M. Colistin: An Update on the Antibiotic of the 21st Century. *Expert Rev. Anti Infect. Ther.* **2012**, *10* (8), 917–934. https://doi.org/10.1586/eri.12.78.
(34) Spapen, H.; Jacobs, R.; Van Gorp, V.; Troubleyn, J.; Honoré, P. M. Renal and Neurological Side Effects of Colistin in Critically Ill Patients. *Ann. Intensive Care* **2011**, *1* (1), 14. https://doi.org/10.1186/2110-5820-1-14.
(35) Seiflein, T. A.; Lawrence, J. G. Two Transsulfurylation Pathways in Klebsiella Pneumoniae. *J. Bacteriol.* **2006**, *188* (16), 5762–5774. https://doi.org/10.1128/JB.00347-06.
(36) Soutourina, O.; Poupel, O.; Coppée, J.-Y.; Danchin, A.; Msadek, T.; Martin-Verstraete, I. CymR, the Master Regulator of Cysteine Metabolism in *Staphylococcus Aureus* , Controls Host Sulphur Source Utilization and Plays a Role in Biofilm Formation. *Mol. Microbiol.* **2009**, *73* (2), 194–211. https://doi.org/10.1111/j.1365-2958.2009.06760.x.
(37) Kanehisa, M. KEGG: Kyoto Encyclopedia of Genes and Genomes. *Nucleic Acids Res.* **2000**, *28* (1), 27–30. https://doi.org/10.1093/nar/28.1.27.
(38) Lithgow, J. K.; Hayhurst, E. J.; Cohen, G.; Aharonowitz, Y.; Foster, S. J. Role of a Cysteine Synthase in Staphylococcus Aureus. *J. Bacteriol.* **2004**, *186* (6), 1579–1590. https://doi.org/10.1128/JB.186.6.1579-1590.2004.
(39) Sievers, F.; Higgins, D. G. Clustal Omega for Making Accurate Alignments of Many Protein Sequences: Clustal Omega for Many Protein Sequences. *Protein Sci.* **2018**, *27* (1), 135–145. https://doi.org/10.1002/pro.3290.
(40) Gouet, P.; Courcelle, E.; Stuart, D.; Metoz, F. ESPript: Analysis of Multiple Sequence Alignments in PostScript. *Bioinformatics* **1999**, *15* (4), 305–308. https://doi.org/10.1093/bioinformatics/15.4.305.
(41) Vaara, M. Agents That Increase the Permeability of the Outer Membrane. *Microbiol. Rev.* **1992**, *56* (3), 395–411.
(42) Meletiadis, J.; Pournaras, S.; Roilides, E.; Walsh, T. J. Defining Fractional Inhibitory Concentration Index Cutoffs for Additive Interactions Based on Self-Drug Additive Combinations, Monte Carlo Simulation Analysis, and In Vitro-In Vivo Correlation Data for Antifungal Drug Combinations against Aspergillus Fumigatus. *Antimicrob. Agents Chemother.* **2010**, *54* (2), 602–609. https://doi.org/10.1128/AAC.00999-09.
(43) Hulanicka, M. D.; Hallquist, S. G.; Kredich, N. M.; Mojica-A, T. Regulation of O-Acetylserine Sulfhydrylase B by L-Cysteine in Salmonella Typhimurium. *J. Bacteriol.* **1979**, *140* (1), 141–146.
(44) Villagra, N. A.; Valenzuela, L. M.; Mora, A. Y.; Millanao, A. R.; Saavedra, C. P.; Mora, G. C.; Hidalgo, A. A. Cysteine Auxotrophy Drives Reduced Susceptibility to Quinolones and Paraquat by Inducing the Expression of Efflux-Pump Systems and Detoxifying Enzymes in S. Typhimurium. *Biochem. Biophys. Res. Commun.* **2019**, *515* (2), 339–344. https://doi.org/10.1016/j.bbrc.2019.05.122.
(45) Burkhard, P.; Tai, C.-H.; Ristroph, C. M.; Cook, P. F.; Jansonius, J. N. Ligand Binding Induces a Large Conformational Change in O-Acetylserine Sulfhydrylase from Salmonella

Typhimurium. *J. Mol. Biol.* **1999**, *291* (4), 941–953. https://doi.org/10.1006/jmbi.1999.3002.
(46) Burkhard, P.; Jagannatha Rao, G. S.; Hohenester, E.; Schnackerz, K. D.; Cook, P. F.; Jansonius, J. N. Three-Dimensional Structure of O-Acetylserine Sulfhydrylase from Salmonella Typhimurium. *J. Mol. Biol.* **1998**, *283* (1), 121–133. https://doi.org/10.1006/jmbi.1998.2037.
(47) Burkhard, P.; Tai, C.-H.; Jansonius, J. N.; Cook, P. F. Identification of an Allosteric Anion-Binding Site on O-Acetylserine Sulfhydrylase: Structure of the Enzyme with Chloride Bound. *J. Mol. Biol.* **2000**, *303* (2), 279–286. https://doi.org/10.1006/jmbi.2000.4109.
(48) Spyrakis, F.; Felici, P.; Bayden, A. S.; Salsi, E.; Miggiano, R.; Kellogg, G. E.; Cozzini, P.; Cook, P. F.; Mozzarelli, A.; Campanini, B. Fine Tuning of the Active Site Modulates Specificity in the Interaction of O-Acetylserine Sulfhydrylase Isozymes with Serine Acetyltransferase. *Biochim. Biophys. Acta BBA - Proteins Proteomics* **2013**, *1834* (1), 169–181. https://doi.org/10.1016/j.bbapap.2012.09.009.
(49) *CLSI. Performance Standards for Antimicrobial Susceptibility Testing. 29th Ed. CLSI Supplement M100. Wayne, PA: Clinical and Laboratory Standards Institute; 2019*.
(50) Donofrio, G.; Franceschi, V.; Capocefalo, A.; Cavirani, S.; Sheldon, I. M. Bovine Endometrial Stromal Cells Display Osteogenic Properties. *Reprod. Biol. Endocrinol.* **2008**, *6* (1), 65. https://doi.org/10.1186/1477-7827-6-65.
(51) Kabsch, W. *XDS*. *Acta Crystallogr. D Biol. Crystallogr.* **2010**, *66* (2), 125–132. https://doi.org/10.1107/S0907444909047337.
(52) Winn, M. D.; Ballard, C. C.; Cowtan, K. D.; Dodson, E. J.; Emsley, P.; Evans, P. R.; Keegan, R. M.; Krissinel, E. B.; Leslie, A. G. W.; McCoy, A.; McNicholas, S. J.; Murshudov, G. N.; Pannu, N. S.; Potterton, E. A.; Powell, H. R.; Read, R. J.; Vagin, A.; Wilson, K. S. Overview of the *CCP* 4 Suite and Current Developments. *Acta Crystallogr. D Biol. Crystallogr.* **2011**, *67* (4), 235–242. https://doi.org/10.1107/S0907444910045749.
(53) Emsley, P.; Lohkamp, B.; Scott, W. G.; Cowtan, K. Features and Development of *Coot*. *Acta Crystallogr. D Biol. Crystallogr.* **2010**, *66* (4), 486–501. https://doi.org/10.1107/S0907444910007493.
(54) Murshudov, G. N.; Skubák, P.; Lebedev, A. A.; Pannu, N. S.; Steiner, R. A.; Nicholls, R. A.; Winn, M. D.; Long, F.; Vagin, A. A. *REFMAC* 5 for the Refinement of Macromolecular Crystal Structures. *Acta Crystallogr. D Biol. Crystallogr.* **2011**, *67* (4), 355–367. https://doi.org/10.1107/S0907444911001314.
(55) Krissinel, E. Enhanced Fold Recognition Using Efficient Short Fragment Clustering. *J. Mol. Biochem.* **2012**, *1* (2), 76–85.
(56) Evans, P. R.; Murshudov, G. N. How Good Are My Data and What Is the Resolution? *Acta Crystallogr. D Biol. Crystallogr.* **2013**, *69* (7), 1204–1214. https://doi.org/10.1107/S0907444913000061.

TABLE OF CONTENT (TOC)

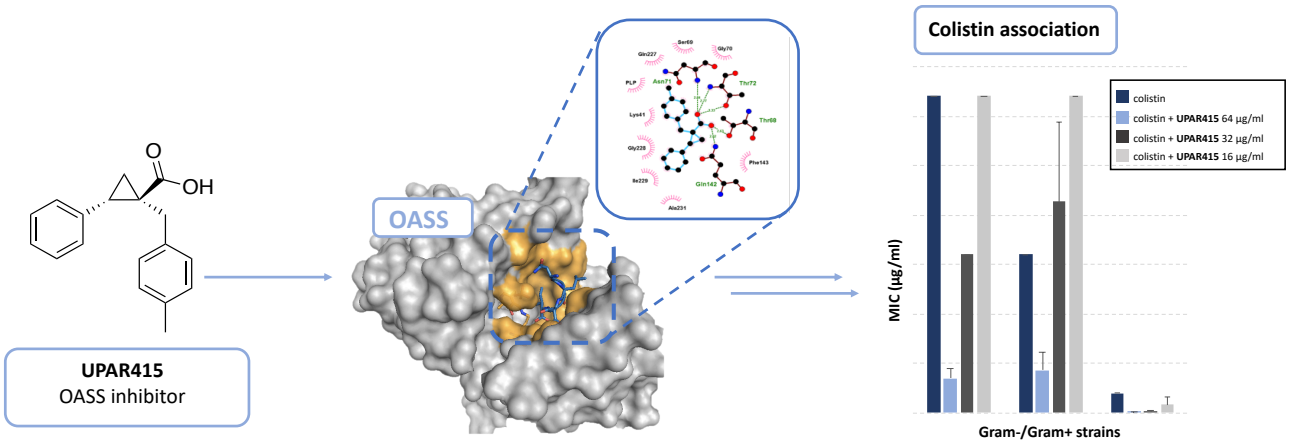
O
OH
UPAR415
OASS inhibitor
OASS
Colistin association
colistin
colistin + UPAR415 64 µg/ml
colistin + UPAR415 32 µg/ml
colistin + UPAR415 16 µg/ml
MIC (µg/ml)
Gram-/Gram+ strains